

## Undulating and crossing axons in the corpus callosum may explain the overestimation of axon diameters with ActiveAx

Tim B Dyrby<sup>1</sup>, Mark Burke<sup>2</sup>, Daniel C Alexander<sup>3</sup>, and Maurice Ptito<sup>1,4</sup>

<sup>1</sup>Danish Research Centre for Magnetic Resonance, Copenhagen University Hospital Hvidovre, Hvidovre, Denmark, <sup>2</sup>Departments of Physiology and Biophysics, Howard University, Washington, United States, <sup>3</sup>Centre for Medical Image Computing, University College London, London, United Kingdom, <sup>4</sup>School of Optometry, University of Montreal, Montreal, Canada

**INTRODUCTION:** Diffusion weighted Imaging (DWI) uses the random motion of water molecules to reveal specific geometrical features of tissue microstructure, i.e. axon diameter (AD) and density indices. Examples of such models are the minimal model of white matter diffusion (MMWMD) i.e. ActiveAx<sup>1</sup> and AxCaliber<sup>2</sup>. When compared with electron microscopy (EM), AD indices obtained from DWI compare favourably in terms of contrast although overestimated with discrepancies at the micro- and macroscopic level. At the microscopic level, DWI does not provide true axon diameters as with EM but volume weighted estimates as larger axons contribute more to the signal than smaller axons<sup>3</sup>.

At the macroscopic level, non-straight axons i.e. fibre dispersion is believed to bias the indices toward higher values as the cross sectional area of non-straight axons appears increased<sup>4</sup>. Finally, scanner hardware and the sequence used can constrain the reliable detection of a range of AD e.g. the smallest axons smaller than a given boundary when using the PGSE sequence<sup>5</sup>. In this study, we validate axon diameter indices from ActiveAx against microstructural and macroscopic anatomical features displayed with EM and classical histology. We identify anatomical features in EM and histology that potentially explain the observed discrepancies when compared with DWI determined AD.

**METHOD:** EM, histology and DWI analysis included each, one fixated monkey brain prepared as described in<sup>6,7</sup>. All procedures were approved by the St Kitts animal care committee under the auspices of the Canadian council on animal care (ccac).

**DWI** was performed on 4.7T experimental Agilent MR scanner using a pulsed-gradient spin-echo (PGSE) sequence with single line-readout. The ActiveAx protocol was optimised<sup>3</sup> for a Gmax of 300 mT/m<sup>7</sup> that included three b-values  $b = [2084, 3084, 9550] \text{ s/mm}^2$  acquired as HARDI multi-shells with [103, 106, 80] gradient directions, and 30  $b=0 \text{ s/mm}^2$ . Whole brain coverage ( $0.5^3 \text{ mm}^3$  voxels), TE=36 ms, TR=3500 ms, and prepared as in<sup>7</sup> was acquired in 62 hours. **Data fitting** included the MMWMD ex vivo model in ActiveAx without<sup>3,5</sup> and with handling of fanning fibre effects<sup>6</sup>. Resultant indices were volume weighted axon diameters AD without and with modelling fibre dispersion. **Analysis:** Mid-sagittal CC was identified on  $b=0 \text{ s/mm}^2$  and divided into ten corresponding ROIs as for EM, and mean AD was calculated. **EM analysis** followed LaMantia et al<sup>6</sup> results: Ten tissue samples (ROIs) were punctured across the mid-sagittal corpus callosum (CC) and further divided in ~ 40 small windows ( $125 \times 125 \text{ \mu m}$ ) for EM imaging. Number, geometry, and spatial distribution of individual axons were measured with MicroBrightField stereo investigator program. Mean axon (inner) diameter distributions AD and with volume weighting was calculated. **Histology** included myelin stain: Coronal samples of the mid-sagittal CC were stained for the inspection of macroscopically axonal spatial incoherence.

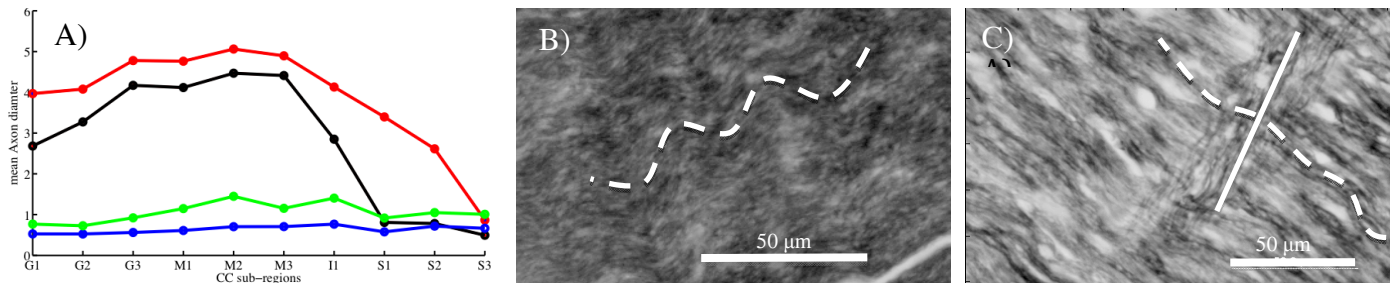


**Figure 1** illustrates axon diameter indices across ten CC sub-regions. A) EM: inner AD with and without volume weighting (green and blue, respectively) and volume weighted AD from ActiveAx with and without fibre dispersion handling (red and black, respectively). B, C) Histology revealed macroscopic non-coherent fibres: Undulating fibres are found across all CC as shown in B) for splenium (example outlined: undulation striped) but in the genu crossing fibres are also found as shown in C) (example outlined: undulation with striped and crossing axons solid).

**RESULTS: Microstructure:** Figure 1 (A, B) shows that mean AD of both EM and DWI clearly follows similar contrast across. Accounting for volume weighting, mean AD of EM clearly increases, but the mean AD of DWI is still shifted toward higher values e.g.  $1.5 \text{ \mu m}$  versus  $5 \text{ \mu m}$  in M2. **Macrostructure:** Figure 1 (C, D) shows histological examples of the existence of non-straight fibres through out CC. Undulating axons can be found throughout CC regions and are typically observed with a wavelength of about  $25 \text{ \mu m}$  and varying undulation amplitude. In the genu only, a small fraction of crossing axons is consistently found. ActiveAx with fibre dispersion modelling<sup>4</sup> account to some extent for macroscopic fibre dispersion effects and produces lower AD estimates than without fibre dispersion modelling. Still, however, the AD of DWI is much higher than EM. Smallest ADs with EM are found in genu but with DWI in splenium.

**DISCUSSION:** Dyrby et al has shown that using the PGSE sequence in combination with limited Gmax smaller AD  $< 2 \text{ \mu m}$  cannot correctly be detected below this boundary<sup>5</sup>. Mean EM axon diameters results and even when accounting for volume weighting were found within this boundary of uncertainty. Nevertheless, AD results from DWI overestimated those of EM as expected<sup>2,3</sup> and were generally shifted toward values higher than those of the boundary where the estimates become imprecise, except for the splenium regions (S1-S3).

With classical histology we observed consistent macrostructural effects in CC that are likely to contribute to the overestimation of axon diameter with DWI. We observed both undulating and crossing axons in CC. Undulating axons has been suggested to influence DTI indices<sup>8</sup>. They will also affect AD estimates because the appearing cross-sectional area of undulating axons will be larger than that for straight axons. Even for the version of ActiveAx that models the dispersion of fibre orientation<sup>4</sup>, undulation is likely to cause overestimation, because the model assumes straight fibres. For large wavelength, this may be a reasonable approximation, but for shorter wavelengths, undulating axons will produce similar diffusion MR signals to larger axons with diameter similar to the undulation amplitude. Similar effect yields crossing fibres, but crossing axons may impact more severely on the appearing cross-sectional area than undulating, and therefore potentially result in much larger appearing AD estimates. This difference between undulating and crossing axons may explain why AD with DWI in genu is larger than in splenium region, and is the opposite result than with that of EM.

**CONCLUSION:** We observed across the whole CC a general spatial homogeneous macroscopic undulating effect, hence its effects on overestimating AD too must somewhat be assumed being a constant factor across CC. This suggests that the axon diameter contrast observed with DWI across CC does coincide with that of EM although the known limitations of the PGSE sequence for small axons. Our results therefore underline the importance of i) developing new sequences so that the smallest axons can be correctly detected in the presence of truly straight axons, and ii) developing a model to relate the axon diameter to the diffusion signal for undulating axons is an open challenge, but one that may well improve axon diameter estimates considerably.

**REFERENCES:** 1) Alexander 2008, *MRM*;60:439–448, 2) Assaf et al 2008, *MRM*;59:1347–1354, 3) Alexander et al, 2010, *NIMG*; 2010;52:1374–1389, 4) Zhang et al, 2011, *NIMG*; 56:1301–1315, 5) Dyrby et al, 2013, *MRM*;70:711–721, 6) LaMantia et al, 1990, *J. Comp. Neurol.*;291:520–537, 7) Dyrby et al 2011, *HBM*;32:544–563, 8) Nilsson et al 2012, *NMR Biomed.*;25:795–805.